

Intricate regimes of propagation of an excitation and self-organization in the blood clotting model

F I Ataullakhanov, E S Lobanova, O L Morozova, E E Shnol',
E A Ermakova, A A Butylin, A N Zaikin

DOI: 10.1070/PU2007v050n01ABEH006156

Contents

1. Introduction	79
2. Mathematical model of blood coagulation	80
3. Methods	81
4. Complex scenarios of the formation of spatially localized standing structures	82
4.1 Introductory notes: standing and moving structures in active media; 4.2 Regions with different regimes in the plane of parameters (K_5 , K_6); 4.3 Two scenarios of peak formation; 4.4 Formation of a stable peak from a decelerating wave; 4.5 Waves decaying after traveling a finite distance; 4.6 Formation of stable peaks from dynamic trigger waves	
5. Complex dynamic regimes in the blood clotting model	86
5.1 Unstable trigger waves and nonstationary regimes; 5.2 Composite waves; 5.3 Splitting waves	
6. Multihump pulses	88
6.1 Appearance of multihump pulses upon a decrease in the inhibitor diffusion coefficient; 6.2 Hypothesis of the multihump pulse origin from bifurcation of trigger waves	
7. Conclusion	90
7.1 Results of the study and the general theory of active media; 7.2 Relation of the results to the current blood coagulation concepts	
References	93

F I Ataullakhanov National Research Center for Hematology, Russian Academy of Medical Sciences, Novyi Zykovskii pr. 4a, 123167 Moscow, Russian Federation Tel./Fax (7-495) 612 88 70

E-mail: fazly@hc.comcor.ru

Physics Department, Lomonosov Moscow State University, Vorob'evy gory, 119992 Moscow, Russian Federation Institute of Theoretical and Experimental Biophysics, Russian Academy of Sciences, 142290 Pushchino, Moscow region, Russian Federation

E S Lobanova National Research Center for Hematology, Russian Academy of Medical Sciences,

Novyi Zykovskii pr. 4a, 123167 Moscow, Russian Federation

O L Morozova Institute of Control Sciences, Russian Academy of Sciences, ul. Profsoyuznaya 65, 117997 Moscow, Russian Federation

E E Shnol' Institute of Mathematical Problems of Biology, Russian Academy of Sciences, ul. Institutskaya 4, 142290 Pushchino, Moscow region, Russian Federation

Tel. (7-4967) 73 37 02

E-mail: emmanuil_shnol@impb.psn.ru

E A Ermakova Semenov Institute of Chemical Physics, Russian Academy of Sciences,

ul. Kosygina 4, 117334 Moscow, Russian Federation

A A Butylin Physics Department, Lomonosov Moscow State University, Vorob'evy gory, 119992 Moscow, Russian Federation

Tel. (7-495) 612 35 22. E-mail: butybuty@yandex.ru

A N Zaikin Institute of Theoretical and Experimental Biophysics, Russian Academy of Sciences,

142290 Pushchino, Moscow region, Russian Federation

Received 26 June 2006, revised 26 July 2006

Uspekhi Fizicheskikh Nauk 177 (1) 87–104 (2007)

Translated by Yu V Morozov; edited by A M Semikhatov

Abstract. A very simple mathematical model of blood coagulation is considered, consisting of a set of three partial differential equations that treat blood as an active (excitable) medium. Many well-known phenomena (running pulses, trigger waves, and dissipative structures) can be observed in such a medium. Recent analytic and numerical results obtained by the authors using this model are presented. The following aspects of the formation of dynamic and static structures in this medium are discussed: (1) three scenarios of the formation of spatially localized standing structures (peaks) observed in the model, (2) complex dynamical modes induced by unstable trigger waves, some of the modes leading to unattenuated activity (dynamical chaos) in the entire space, and (3) a new type of excitation propagation in active media—stable multihumped peaks due to trigger wave bifurcation—predicted by the model.

1. Introduction

Media containing energy sources at each point in space display a wonderful diversity of dynamic behavior and self-organization. It is becoming increasingly clear that such systems are not exceptional: more and more examples of them are emerging as researchers gain a deeper insight into the nature of complex systems, both chemical and physical. This is especially true of biological systems, which are intrinsically far from equilibrium and have energy sources distributed throughout the entire medium space.

Investigations into events occurring in such media, frequently referred to as active media, are important in many natural sciences. The general theory of active media

remains to be formulated, and practically each in-depth study reveals new types of their dynamics and self-organization. There is no reason to think that these types are unique; on the contrary, the available experience indicates that, once described, a new dynamic regime or bifurcation is thereafter found in other systems, even those that have been investigated for a long time.

We have recently demonstrated [1–7] that blood can be regarded as an active (excitable) medium for the purpose of coagulation studies. Primary excitation is induced by an injury to the wall of a blood vessel, and the ‘coagulation wave’ spreading deeper into the vessel is analogous to autowaves inherent in active media. Blood coagulation is a combination of a few dozen inter-related biochemical reactions leading to the rapid formation of a hard polymer in the blood flow near the injured wall. It is a highly complicated process from the standpoint of nonlinear dynamics and self-organization. A unique property of blood as an active medium is that a self-sustained wave of thrombin, the enzyme responsible for thrombus formation, travels only a finite distance. This fact is paramount for the coagulation process because the clot must remain at the lesioned site.

The dynamical characteristics of blood plasma as an active medium have been investigated using mathematical models differing in terms of detailedness and based on current concepts of molecular mechanisms underlying blood clotting. It has been shown that the simplest model containing only three differential equations [6] fairly well describes many dynamic properties of the real blood coagulation process. These results were reviewed in much detail in our paper published in *Physics – Uspekhi* in 2002 [8]. Further studies of a spatially one-dimensional variant of this model have revealed a number of unusual regimes of excitation propagation and self-organization, to be considered in this paper. These are various regimes of the development of stationary standing structures from running waves, pulses that split during propagation and create spatio-temporal chaos, and complex wave pictures generated by unstable trigger waves that transform one spatially homogeneous state into another. These regimes may be of interest to many researchers of biological, physical, and chemical processes. In our work reported in this paper, we examined these phenomena on large time and space scales within a relatively wide region of the parameter space. First and foremost, we sought to gain insight into the nature of the regimes being investigated rather than understand how close they are to the real blood clotting process.

Some of these phenomena were observed by researchers using quite different physical or physico-chemical models (references to their publications are given in the text below). Others seem to have been first observed in our studies. In the cases where the mathematical nature of the phenomena of interest can be clarified, we present the results of analysis with emphasis on their relation to the bifurcation theory.

The paper is organized as follows. Sections 2 and 3 describe the model and methods of numerical experiments. In Section 4, various scenarios of the formation of localized standing structures are discussed. Section 5 deals with dynamic regimes differing in terms of complexity. Section 6 is focused on the origin of complex-shaped running pulses propagating in a regular manner, that is, with constant velocity and without change in shape.

In all cases, we were interested in the processes proceeding under standard excitation of the medium, i.e., at a local

(within a small region) increase in the thrombin concentration. Such excitation simulates a real situation associated with an injury to the vascular wall.

General conclusions to which we attach special importance are formulated in the first part of Section 7. Its second part relates the results obtained in the framework of the simplified model to the current blood coagulation concepts.

2. Mathematical model of blood coagulation

The simplest blood coagulation model is a three-component set of differential equations of the reaction–diffusion type. Its derivation and the analysis of the simplest regimes are described at length in our earlier works [6, 8].

In this paper, we primarily consider phenomena observed in spatially one-dimensional systems. The one-dimensional version of the blood clotting model being considered has the form

$$\begin{aligned}\frac{\partial u_1}{\partial t} &= D_1 \frac{\partial^2 u_1}{\partial x^2} + K_1 u_1 u_2 (1 - u_1) \frac{1 + K_2 u_1}{1 + K_3 u_3} - u_1, \\ \frac{\partial u_2}{\partial t} &= D_2 \frac{\partial^2 u_2}{\partial x^2} + u_1 - K_4 u_2, \\ \frac{\partial u_3}{\partial t} &= D_3 \frac{\partial^2 u_3}{\partial x^2} + K_5 u_1^2 - K_6 u_3.\end{aligned}\quad (1)$$

In the absence of diffusion terms, Eqns (1) become

$$\begin{aligned}\frac{du_1}{dt} &= K_1 u_1 u_2 (1 - u_1) \frac{1 + K_2 u_1}{1 + K_3 u_3} - u_1, \\ \frac{du_2}{dt} &= u_1 - K_4 u_2, \\ \frac{du_3}{dt} &= K_5 u_1^2 - K_6 u_3,\end{aligned}\quad (2)$$

where u_1 is the concentration of the activator (thrombin), u_2 is the concentration of the accelerator of activator formation (activated factor XIa), and u_3 is the concentration of the inhibitor (activated protein C). More precisely, the variables u_k are dimensionless concentrations of these substances. Both the inhibitor and the accelerator appear at a given point only in the presence of the activator. All three substances have almost identical diffusion coefficients, and hence almost all the results were obtained in the case where their values were taken equal. The equations involve six constants K_i that characterize the ‘chemical’ part of the system. These constants are complex combinations of quantities used to normalize concentrations and constants of chemical reactions underlying blood coagulation.

It follows from Eqns (1) that the constants K_2 and K_3 are dimensionless, while the values of the four remaining constants K_i and diffusion coefficients D_k depend on the choice of the units of measure. To facilitate comparison with our results in [1–7, 9–11], we here use the same time unit as in Ref. [6], $t_0 = 0.435$ min. The unit of length l_0 was chosen such that at a given t_0 , numerical values of all identical diffusion coefficients are equal to unity [9–11]. At the initial value of $D = 0.0006$ mm² min^{−1}, this gives $l_0 = 0.0161$ mm. These units of length and time are used in Sections 4–6, where the results of numerical experiments with model (1) are presented. The values of ‘chemical’ constants K_i reasonably corresponding to the experimental data are given separately in each of Sections 4–6.

A hard blood clot is formed as a result of the thrombin-catalyzed production of specialized protein fibrin; therefore, the time integral of u_1 describes spatial dynamics of clot growth.

Model (1) at all positive values of the parameters K_i and D_i always has a trivial solution $u_k(x, t) \equiv 0$. This solution is stable in the sense that if all $u_k(x, t)$ are small at $t = 0$, then they exponentially tend to zero in the course of time.

Model (1) exhibits threshold properties, i.e., the appearance of nontrivial transient and stationary regimes when the initial excitation of the variable u_1 is relatively high (has an overthreshold value) and the segment at which this excitation is given is not too small.

In the one-dimensional case, the model reproduces regimes characteristic of active media, viz. *autowaves*, *trigger waves*, and *peaks*. By *autowaves*, we mean spatially localized pulses that propagate with a constant velocity and without change of shape. We occasionally call them pulses. *Trigger waves* are the waves propagating at a constant velocity and without change of shape that switch over the medium from one spatially homogeneous stable state to another. Trigger waves that eventually transform the medium from the initial (trivial) spatially homogeneous stable state into a different (nontrivial) spatially homogeneous stable state are called *switch-on waves* in what follows. Accordingly, waves that bring the medium back to the initial state are *switch-off waves*. By *peaks*, we mean spatially localized standing structures. In the model being considered, these structures are usually shaped like peaks, each corresponding to a local increase in concentrations within a rather narrow region (hence, their name). Sometimes, such structures consist of a series of regularly distributed peaks.

Model (2) has three standing solutions in many regions of the parameter space: the trivial solution (where all u_k are equal to zero) and two with nonzero (positive) values of the variables. The fixed singular point $(0, 0, 0)$ is always a stable node. The types and positions of the remaining singular points vary as the parameters are changed. The solutions of model (1) describing spatially homogeneous states of a medium correspond to these singular points. In what follows, a medium having a single spatially homogeneous stable (trivial) state is said to be *monostable* and that with two spatially homogeneous stable states (trivial and nontrivial) is said to be *bistable*. Spatially homogeneous states of system (1) do not differ from the corresponding singular points of system (2) in terms of stability type if all the diffusion coefficients are identical.

In all sections in this paper except Section 6, the three diffusion coefficients are assumed to be equal; hence, stability of spatially homogeneous stationary states can be evaluated from the stability of singular points of 'local' system (2).

3. Methods

In the numerical analysis of model (1) in [6, 9–11], we replaced differential equations with finite-difference ones and the infinite line with a sufficiently long segment. The boundary conditions at the ends of the segment ensured the absence of a flow of each substance (the condition $u'_x = 0$). The standard initial conditions were defined as follows: $u_1(x, 0) = \bar{u}_1$ within a small segment and $u_1(x, 0) = 0$ outside it; $u_2(x, 0) = 0$ and $u_3(x, 0) = 0$ at all x . At the chosen normalization of concentrations (see Section 2), the quantity u_1 does not exceed 1, and we usually assumed \bar{u}_1 to be equal to 0.2.

Calculation of time-independent solutions of system (1), which were identified by the onset of a stationary regime, was performed until deviations of the values of the first component u_1 ($0 < u_1 < 1$) in the current time interval from the corresponding values in the preceding time interval became smaller than 10^{-5} .

The relevant stationary regimes (standing peaks and waves propagating with constant velocity without changing shape) can be found by solving ordinary differential equations. Stationary-wave solutions (autowaves and trigger waves) were found by solving the nonlinear boundary value problem

$$\begin{aligned} D_1 v_1'' + c v_1' + K_1 v_1 v_2 (1 - v_1) \frac{1 + K_2 v_1}{1 + K_3 v_3} - v_1 &= 0, \\ D_2 v_2'' + c v_2' + v_1 - K_4 v_2 &= 0, \\ D_3 v_3'' + c v_3' + K_5 v_1^2 - K_6 v_3 &= 0, \\ v_1'(0) = v_2'(0) = v_3'(0) = v_1'(L) = v_2'(L) = v_3'(L) &= 0, \end{aligned} \quad (3)$$

where

$$u_k(x, t) = v_k(x - ct). \quad (3a)$$

Peaks were found by solving the same nonlinear boundary value problem at $c = 0$. For peaks, the unknowns are the three functions $v_k(x)$ that determine the profile; for waves, the unknowns are the three functions $v_k(x)$ determining the wave profile and the wave velocity c . By solving ordinary differential equations, waves and peaks can be found more accurately than by observing the time evolution of the solution of the original equations (1). This also allows doing what cannot be done by direct solution of system (1)—finding unstable wave profiles and velocities or profiles of unstable standing peaks. The segment length L must be large enough if wave behavior on the infinite line is to be accurately described.

The nonlinear boundary value problems for ordinary differential equations (3) were solved by iterations using Newton's method, with one linear boundary value problem solved at each iteration. To be precise, the situation was as follows. The problem of finding a wave of a given type on the infinite line has translational invariance; hence, the corresponding (homogeneous) linearized problem has a nonzero solution. The linearized boundary value problem on a segment of a large length L is then close to degeneration, and the direct application of Newton's method is impossible in this case. To eliminate the (approximate) translational invariance, we introduced an additional condition in the middle of the segment $[0, L]$. Specifically, the calculation of autowave profiles implied the condition $v_1'(L/2) = 0$, fixing the position of the first-variable maximum. The necessity of an extra condition directly ensues from the consideration of finite-difference equations. It follows that the problem involves an additional 'unknown' parameter (wave velocity); therefore, an additional condition must be imposed to make the number of equations equal to the number of unknown quantities. Linear boundary value problems with an additional 'boundary' condition in the middle of the segment have good properties and can be solved by standard methods [12–14]. We used a special approach to accelerate computation. The solution obtained previously at close parameter values served as the first approximation. For the initial parameter values, the solution eventually established in system (1) after a

rather long time was taken as the first approximation. Naturally, the initial parameter values were chosen in the region including stable autowaves or standing peaks. Solutions found at other parameter values were checked for stability as follows. A solution obtained by Newton's method was weakly perturbed and used as the initial condition for system of equations (1). Unstable solutions did not 'survive' during calculations, unlike stable ones that 'survived.'

4. Complex scenarios of the formation of spatially localized standing structures

4.1 Introductory notes: standing and moving structures in active media

Of special interest in the context of the blood coagulation process are dynamic regimes in which excitation does not propagate far from the initial activation area. The simplest regime of this type is represented by rapidly decaying excitation. In this case, the excitation area is practically immobile. This trivial regime is observable in a variety of media. Much more interesting are two other excitation regimes in which a pulse begins to propagate from the activation site at the initial instant. Its velocity and amplitude do not significantly change until the pulse stops at a certain distance from its origin. Thereafter, the pulse either decays (regime 1) or continues to exist in the form of a standing localized peak (regime 2). As mentioned in Section 2, the clot produces fibrin in a concentration proportional to the time integral of the variable u_1 . It is therefore understandable that these two regimes correspond to the normal (spatially bounded) development of the clot in response to vascular damage. We note that both regimes are excited by a local increase in the thrombin level over a small part of the segment. Such type of activation adequately simulates blood clotting conditions in the body. For this reason, just this type is meant by the term 'standard activation' (or 'standard initial conditions') used below when differential equations are considered. Regime 1 (a pulse traveling rather far from the excitation area before it decays) is known to be described by many sets of equations having autowave solutions. In contrast, regime 2 is an unusual scenario of peak formation at a certain distance from the activation site described recently in Refs [6, 9].

Stable standing peaks are among the most interesting phenomena in active reaction–diffusion media. Such a peak is a structure in which stationary concentrations of medium components are quite different from the corresponding concentrations in the remaining space. Despite free diffusion, such a 'spot' does not spread with time, remaining resistant to perturbations and able to restore its size and shape. Koga and Kuramoto [15] first demonstrated the formation of such a structure at the activation spot or as the result of a collision between oppositely directed trigger waves in a reaction–diffusion model (piecewise-linear version of the system of two equations with a cubic nonlinearity of the FitzHugh–Nagumo (FHN) type [16]). Similar structures were later studied in many works reviewed and analyzed in Ref. [17]. These studies showed that stable standing peaks may arise in the simplest bicomponent models if the diffusion coefficient of the inhibitor is much higher than that of the activator. Later, standing peaks in a model with the piecewise-linear approximation of cubic nonlinearity [18]

were described for a wider range of ratios of the activator and inhibitor diffusion coefficients, including the unit value (at equal coefficients). However, Ref. [16] lacks analysis of peak stability. In this work, as in those mentioned above (see the references in [17]), stable peaks occurred *at the excitation site*. But we found that in a blood clotting model, peaks may arise *far from the excitation region* because they originate from a wave closely resembling an autowave [6]. We compared the model being considered here and a modified FHN model and concluded that the latter may contain many of the regimes described in Sections 4–6.

Bifurcations that convert various standing structures into moving ones have been studied by different authors. Schuetz et al. [19] considered a bifurcation resulting in the transition from a standing strip to a moving one in a two-dimensional model. Zaikin first described traveling localized structures in a two-dimensional active medium model (Zaikin's exciton) [20, 21]. Schenk et al. [22, 23] studied moving and stationary structures in a similar model.

More than ten years after the publication of Refs [20, 21], similar excitons were obtained by Poptsova in another model system of differential equations [24]. This author reproduced the numerical experiments by Zaikin that had demonstrated the dual (particle–wave) properties of a macroexciton: in a head-on collision, two wave–particles either annihilate or are re-emitted in the direction perpendicular to their original direction; in the interaction at displaced opposite courses, they are re-emitted at a certain angle; and they merge if their trajectories cross at an angle smaller than a certain critical angle. Poptsova showed that the existence of spatially localized autowave solutions is not an exceptional feature of the Zaikin model [20, 21].

Bifurcations of the transition from a standing peak to an autowave in the one-dimensional case and a stably standing spot to a moving spatially localized one in the two-dimensional case were described by a more complicated three-component system of equations [25]. Besides stable and unstable peaks, localized structures in the form of oscillating peaks were discovered in certain models. Regimes of such types usually arise and disappear as a result of the cycle birth bifurcation (Andronov–Hopf bifurcation) [26]. For example, it was shown that peaks in models of the FHN type lose stability under the Andronov–Hopf bifurcation [15]. To elucidate the mechanism of peak formation far from the activation site, we examined the parameter region of the existence of stable peaks in model (1) and bifurcations at the boundaries of this region.

4.2 Regions with different regimes in the plane of parameters (K_5, K_6)

The results of numerical experiments analyzed in great detail in this section and in Sections 4.3–4.6 were first presented in Refs [6, 9]. In spatially one-dimensional system (1), a standing peak can exist in a relatively large region of the parameter space. We consider a cross section of the parameter space within the region of the solution existence in the form of stationary peaks in more detail. We take the plane (K_5, K_6) as such a cross section (Fig. 1) at constant values of the remaining parameters shown in Table 1. The rationale for

Table 1.

K_1	K_2	K_3	K_4	K_5	K_6	D
6.85	13.5	2.36	0.078	12.0–24.0	0.02–0.08	1.0

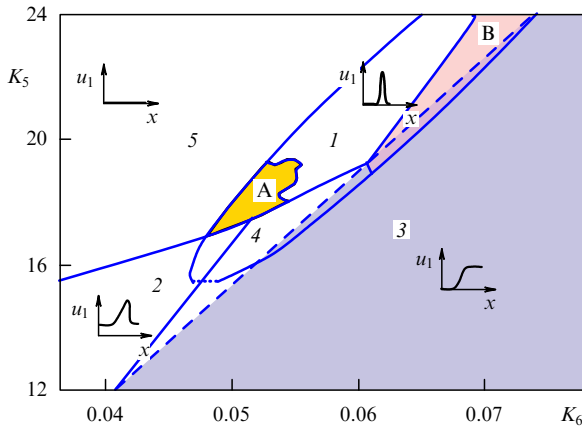


Figure 1. Parametric portrait of system (1) in the plane of parameters (K_5, K_6) at the parameter values given in Table 1. Region 1 where peaks exist is a diagonally elongated ‘ellipse.’ The lower boundary of region 1 (dotted line) is given approximately. Region 1 is partly penetrated by the regions of autowave pulses (2), trigger (or bistability) waves (3), and complex-shaped running pulses (4). Region 5 adjoining region 1 on the left has only a trivial stationary solution. Subregions A and B of region 1 correspond to different peak formation scenarios under standard initial conditions: A — peak formed at a certain distance from the activation site, B — peak formed at the activation site (see the text). The left boundary of bistability region 3 is defined as the line of stability loss by the upper state as a result of the Andronov – Hopf bifurcation (dashed line). Model (2) is bistable everywhere right of the dashed line and monostable left of this line.

the choice of the ranges of model constants can be found in Ref. [6].

Region 1 in Fig. 1 is the set of K_5 and K_6 values at which stable peaks exist. Its boundary is shown by the continuous solid line, except a small boundary portion in the lower part (dotted line) that we did not examine. Region 2 corresponds to stable autowaves. In this region, autowaves occur at the standard initial conditions whenever the excitation exceeds a threshold level. Region 3 is the bistability region in which system 2 has two stable singular points, one being $(0, 0, 0)$ and the other having positive coordinates. In other words, system (1) has two stable solutions independent of x and t when all diffusion coefficients are identical.

The stable state corresponding to the ‘top’ singular point loses stability at the left boundary of region 3 (dashed line) as a result of the Andronov – Hopf bifurcation. Left of this boundary, system (2) has a single stable (trivial) singular point across the entire examined range of parameters. Region 4 contains pulses of complex shape, and region 5 is characterized by the sole stable stationary solution of system (1) at which all $u_k(x)$ are identically equal to zero. Decaying pulses at the boundary between regions 5 and 2 are observed under standard initial conditions.

Model (1) allows different peak formation scenarios (Fig. 2). A peak may arise either at the activation site (Fig. 2a) or far from it (Fig. 2b). It may also result from a complex combination of trigger wave movements away from and into one another (Fig. 2c). We consider these scenarios in more detail. Region 1 contains two subregions, A and B, in which stable peaks develop under the standard initial conditions, although the dynamics of their formation are strikingly different. A peak in subregion A forms after traveling a certain distance from the activation site (Fig. 2b); in region B, it arises at the activation site (Fig. 2a). It can be seen from Fig. 1 that subregions A and B have no common

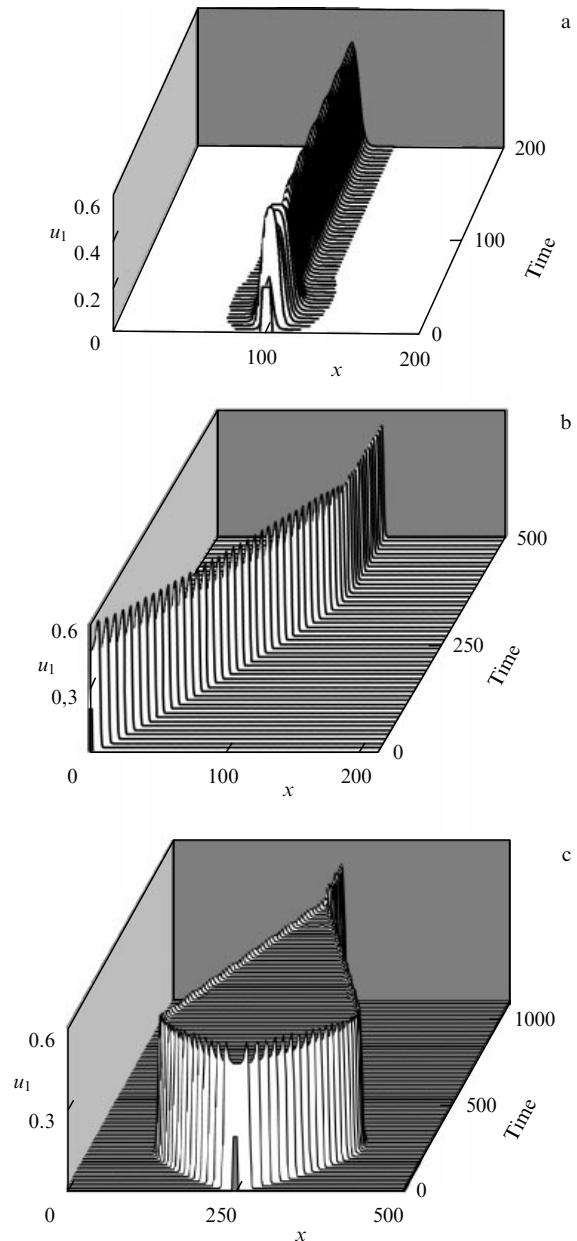


Figure 2. Different peak formation scenarios in the blood coagulation model in response to local overthreshold activation: (a) simple peak formation dynamics — peak formed at the activation site; (b) the first complex scenario of peak formation — excitation first spreads from the activation site as a running pulse but thereafter stops and undergoes conversion to a standing peak; (c) the second complex scenario of peak formation — the excitation area first expands but then narrows and transforms to a standing peak (see the text for details).

boundary. Stable peaks do not develop from the standard initial conditions outside these subregions; they need special initial conditions to form. The entire region where peaks are formed was mapped onto the parameter plane as follows. A peak was found in area A (or B) under standard natural conditions and the functions $u_k(x)$ describing this peak were used as the initial conditions to calculate the solution at the adjacent point of the parameter plane. Moving like this over the parameter plane, we found the entire region of stable peaks. It then became clear that areas A and B are two parts of a large connected region 1 (where peaks exist).

There is a small area where regions 1 (peaks) and 3 (bistability) intersect; in the remaining part of region 1, the

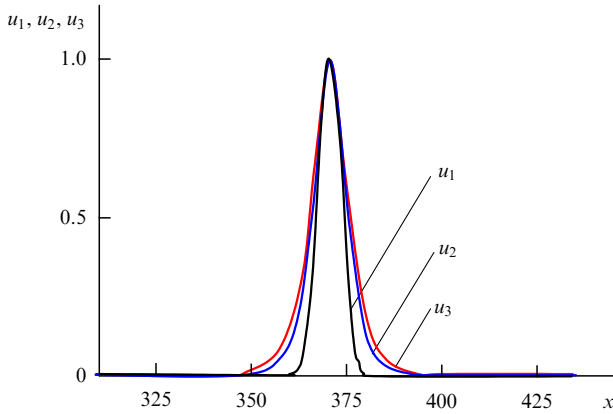


Figure 3. Spatial distribution of variable concentrations in an established peak for scenario 1 of peak formation from the standard initial conditions ($K_5 = 17.255$, $K_6 = 0.050$, see Table 1 for the remaining parameters). The value of each variable u_1 , u_2 , and u_3 is normalized to the maximum concentration: 0.53, 4.29, and 44.90, respectively. The inhibitor concentration u_3 has the largest spatial distribution.

system is monostable. The intersection area of regions 1 and 3 has at least three stable solutions, viz. a lower homogeneous (trivial) solution, an upper homogeneous solution, and an inhomogeneous solution in the form of a standing peak. Region 1 also partly intersects regions 2 (stable autowaves) and 4 (pulses of complex shape). Interestingly, system (1) has solutions in the form of unstable peaks observed throughout the entire examined part of the parameter space (see Fig. 1) including the bistability region and region 1 where stable peaks exist.

4.3 Two scenarios of peak formation

Figure 2b presents a scenario of stable peak formation occurring in subregion A (scenario 1). Under standard activation near the boundary of the segment, a pulse travels away from the origin, then slows down and transforms into a standing peak. At the beginning, the process is reminiscent of autowave propagation but thereafter this quasiwave stops and undergoes conversion to a standing structure. If the standard activation occurs close to the middle of the segment, pulses propagate in different directions and give rise to two peaks.

Figure 3 shows the spatial distribution of all three variables describing a typical peak in region 1. It can be seen that the inhibitor u_3 is characterized by the broadest distribution, which accounts for the stability of the resultant structure. The formation rate of all substances is especially high in the center of the peak, from which they diffuse continuously towards the periphery, where inhibitory reactions predominate. The peak is symmetric in shape, unlike the initial quasiautowave, whose leading edge is much steeper than the trailing one.

Figure 2c illustrates a peak formation scenario in subregion B of the parameter plane (K_5, K_6) (scenario 2) under standard activation conditions in the center of the segment. In this case, the peak formation occurs exactly at the activation site but its dynamics are rather complicated. For example, it can be preceded by the expansion of the excitation area, followed by its narrowing. As can be seen from Fig. 2c, the activation site is the origin of two dynamic switch-on waves that stop after a time and undergo transformation into

two switch-off waves, which start moving in opposite directions. Thereafter, the switch-off waves slow down and interact to form a stable peak. We note that these waves are nonstationary because their shape and velocity constantly change during motion. Hence their name, *dynamic* trigger waves. At large values of the parameter K_5 (in the upper part of area B), the dynamics are of a simpler character, i.e., a peak forms at the activation site without a previous expansion of the excitation area.

It can be seen from the diagram in Fig. 1 that area A adjoins region 2 (autowaves) and area B borders the bistability region. The initial stages of peak formation in area A have the form of running pulses (Fig. 2b) very similar to autowaves existing ‘in the neighborhood.’ The peak arising in the lower part of area B is first reminiscent of a trigger wave but thereafter transforms into a switch-off wave (Fig. 2c). This part adjoins region 3, in which trigger waves exist. The peak formation scenarios in areas A and B therefore seem to be affected by stationary regimes in the adjacent regions of the parameter space. We consider the situation near the boundaries between region 2 and area A and between region 3 and area B in more detail.

4.4 Formation of a stable peak from a decelerating wave

Standard medium activation in area A results in scenario 1 of stable peak formation (Fig. 2b), when a wave-like pulse begins to propagate from the activation site but stops and transforms into a stable peak. The closer the parameter point to the boundary between A and region 2, the greater the distance traveled by the pulse with almost constant velocity and amplitude. Figure 4 shows this distance as a function of K_5 at a fixed K_6 ($K_6 = 0.05$).

We consider the disappearance of stable autowaves as they cross the boundary between regions 2 and A in more detail. Figure 5 shows the dependence of the wave propagation speed on K_5 at the fixed value $K_6 = 0.05$, including the branch of unstable autowaves. As K_5 increases, the autowave speed decreases. At the boundary under consideration, $K_5 = K_{\text{scr}}^{(1)} = 17.247$. At the critical value $K_{\text{scr}}^{(1)}$, the branches

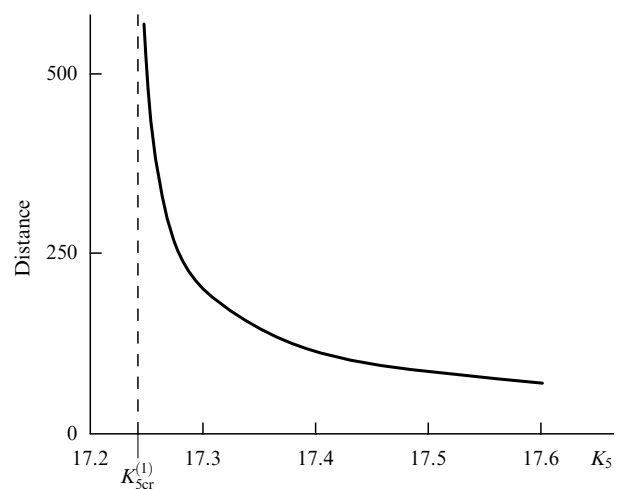


Figure 4. Dependence of the distance traveled by a pulse from the activation site in area A on the parameter K_5 ($K_6 = 0.05$). The pulse was induced by increasing u_1 to an over-threshold value (0.2) at a small section near the left boundary. The distance traveled by the pulse was that from the boundary to the maximum of the developed peak. K_{scr} is the bifurcation value of the parameter below which the region of autowaves lies. The initial excitation in this region gives rise to an autowave.

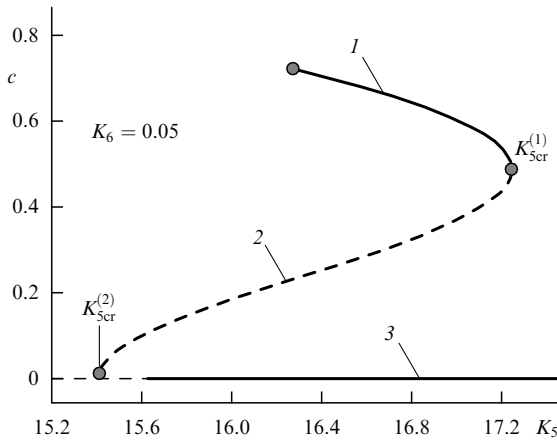


Figure 5. Bifurcation diagram for autowaves and peaks at $K_6 = 0.05$. The limit point $K_{scr}^{(1)} = 17.247$ corresponds to the point of merging between stable and unstable autowaves and the point $K_{scr}^{(2)} = 15.4$ to the intersection of autowaves and peak branches (see text for details).

of stable and unstable autowaves merge with one another and area A contains no autowaves. In other words, the peak formation scenario 1 occurs near the line where stable and unstable autowave branches merge.

Of special interest is the behavior of the unstable autowave branch far from area A. At $K_{scr}^{(2)} = 15.4$ (see Fig. 5), the speed of an unstable autowave decreases to zero and the autowave branch intersects the peak branch (horizontal line 3 in Fig. 5). The line is shown solid where the peaks are stable and dashed where their stability awaits an in-depth analysis. We note that K_5 values for stable autowaves coexisting with stable peaks correspond to a partial overlap between regions 1 and 2. In this overlapping area, a stable autowave arises under the standard initial conditions, whereas stable peaks need special initial conditions to form.

4.5 Waves decaying after traveling a finite distance

The left boundary of region 2 is completely formed by merged branches of stable and unstable autowaves. The following process develops from the standard initial conditions in region 5 close to its boundary with region 2. First, a pulse propagates for a certain time at a roughly constant speed and barely changes its shape. Thereafter, its motion slows down. In contrast to the case described in Section 4.4, no stationary standing structure develops, the pulse decays, and the medium relaxes toward a trivial spatially homogeneous state. The bifurcation diagram depicting autowaves and peaks at a fixed K_6 for this portion of the boundary of region 2 resembles the bifurcation diagram shown in Fig. 5. The farther the parametric point lies from the boundary of region 2, the smaller the distance at which the pulse decays; in contrast, the distance traveled by the pulse infinitely increases closer to the autowave region as in the case of peak formation in area A.

Thus, the general property of the external surroundings of region 2 close to the lines corresponding to bifurcation of merging between stable and unstable autowaves is the ‘dynamic memory’ of lost autowaves: an autowave-like structure is the first to form in response to the standard excitation. Because the region contains no stable autowaves, this structure travels a certain distance and starts to transform into a stable object characteristic of the given region. In

the presence of stable peaks, the wave is converted into a standing peak. If the trivial homogeneous state is the sole one in the region, the wave decays. The closer the system to the boundary of the autowave region, the better the ‘memory,’ that is, the longer the wave lifetime and the distance traveled.

4.6 Formation of stable peaks from dynamic trigger waves

The complex regime of stable peak formation mentioned in Section 4.3 is observed in the lower part of area B, where the trivial spatially homogeneous state and stable peaks coexist with stable switch-on waves (see Section 2, where definitions are given). Stable switch-off waves appear at the exit from area B through its right boundary; the proximity of their existence region to area B is apparent at the early stages of peak formation. We consider model behavior during the transition from area B to region 3 and limit ourselves to the variation of a single parameter, as before.

In this analysis, we fixed $K_5 = 20$ and characterized trigger waves by their speed, assigning the respective signs plus and minus to the speeds of switch-on and switch-off waves. The resulting bifurcation diagram is presented in Fig. 6. The dependence of the speed on K_6 is S-shaped and consists of three branches. The branches of stable and unstable switch-on waves are depicted by the solid and dashed lines, respectively. At $K_5 = 20$, there is a small interval of values in which three branches of solutions in the form of trigger waves coexist: these are two stable branches shown by the solid line and linked by the unstable branch (dashed line). The horizontal straight line $c = 0$ corresponds to the solutions in the form of peaks. The continuous portion of this line corresponds to stable peaks. Arrows indicate the limits within which the standard initial conditions lead to the formation of a stable peak at the activation site.

Interesting dynamics are observed for K_6 values close to $K_{6cr}^{(1)}$ ($K_6 < K_{6cr}^{(1)}$). This parameter range incorporates only two

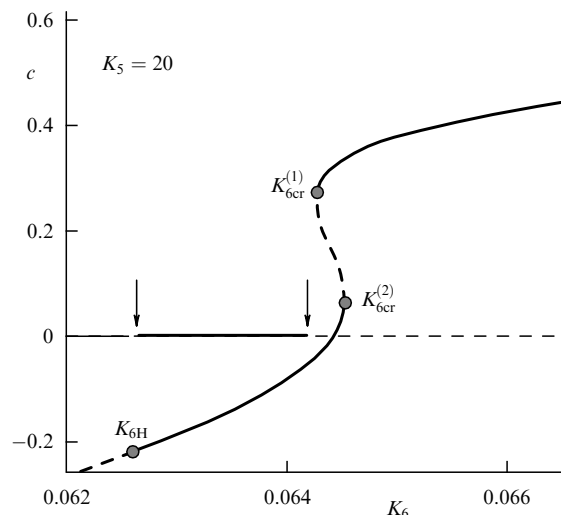


Figure 6. Bifurcation diagram for trigger waves and peaks obtained by varying the parameter K_6 at the fixed value $K_5 = 20$. The bottom circle corresponds to the value $K_{6H} = 0.0626$, at which the upper singular point of system (2) loses stability due to the Andronov–Hopf bifurcation; $K_6 > K_{6H}$ is associated with bistability. Switch-on and switch-off waves coexist in a certain range $K_6 > K_{6cr}^{(1)}$. For $K_6 < K_{6cr}^{(1)}$, bistability coexists with stable peaks. The region where peaks exist is shown by a horizontal line at the zero speed level. Arrows indicate the area in which peaks arise under the standard initial conditions.

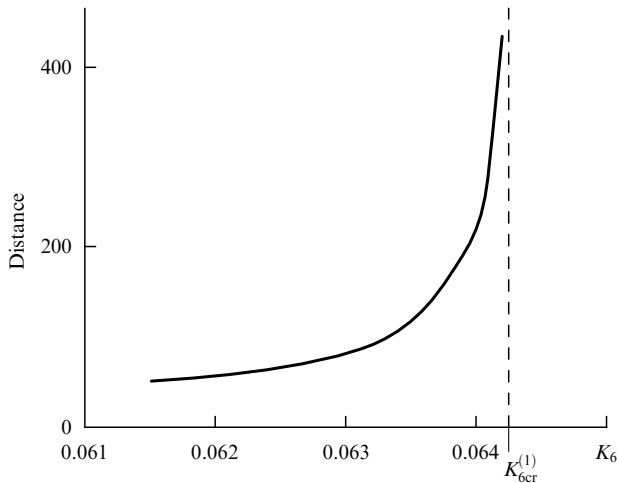


Figure 7. Dependence of the distance traveled by a pulse from the activation site in area B on the parameter K_6 (at $K_5 = 20$). The distance was computed from the motion of a point on the wave front at the height given by half the level u_1 of the upper spatially homogeneous stable state and determined at the instant of maximum expansion of the excitation zone.

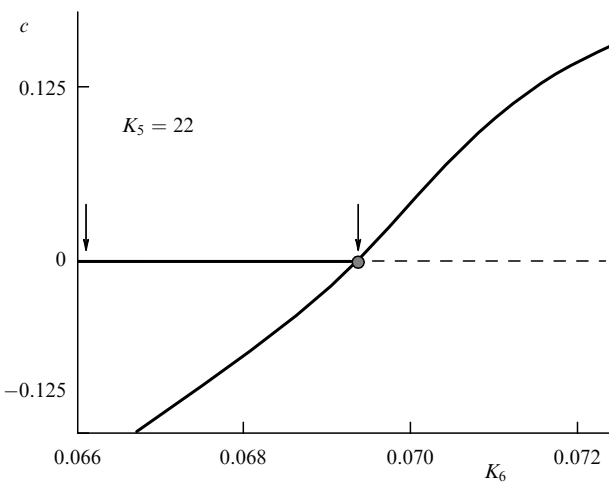


Figure 8. Bifurcation diagram for trigger waves obtained by varying the parameter K_6 ($K_5 = 22$).

types of stable solutions, switch-off waves and peaks. Standard activation in the center of the segment might be expected to make the system form one of the solutions immediately. Instead, dynamic switch-on waves appear first; they start propagating long enough, then stop and transform into switch-off waves (Fig. 2c). As the switch-off waves come closer to one another, they interact and give rise to a stable peak. It was first shown in Ref. [26] that interacting switch-off waves do not necessarily annihilate. The distance traveled by dynamic switch-off waves increases as K_6 approaches $K_{6cr}^{(1)}$ (Fig. 7). It can be seen from Fig. 6 that the branch of stable switch-on waves disappears as it merges with the branch of unstable switch-on waves at $K_6 = K_{6cr}^{(1)}$. The speeds of merging waves differ from zero. The situation near the line where they merge at the boundary between regions B and 3 resembles that near the line where autowaves merge as described in Section 4.4. The processes occurring in either case close to the boundary have initial stages resembling the regimes characteristic of the adjacent regions. Here, close to

the boundary of area B, the process starts as a pair of propagating switch-on waves.

In area B, the S-shaped portion of the bifurcation diagram decreases with increasing the parameter K_5 until the curve becomes monotonic (Fig. 8). Simultaneously, the increase in K_5 is accompanied by a decrease in the primary excitation area. The initial phase (propagation of switch-on waves) becomes inconspicuous and peak formation is confined to the activation site. The right boundary of the stable-peak region turns into the line corresponding to sign reversal of the trigger wave speed (on this line, switch-on waves undergo conversion to switch-off waves).

5. Complex dynamic regimes in the blood clotting model

The results presented in this section were first obtained in [10].

5.1 Unstable trigger waves and nonstationary regimes

As shown above, model (1) is bistable in a certain range of parameters when all diffusion coefficients are equal; in other words, it encompasses two coexisting stable spatially homogeneous states, lower (trivial) and upper. At these parameters, the model contains trigger waves that transform the medium from one homogeneous state to another. There is a region in the parameter space in which the upper state still exists after it loses stability. Interesting solutions may be expected in this region. Dynamic regimes found in model (1) are considered in Sections 5.2, 5.3, and 6.

Naturally, stable trigger waves cannot exist when the upper spatially homogeneous state loses stability. Nevertheless, it is possible to find solutions of stationary system (3) in the form of trigger waves (if they are still present). Remarkably, the front parts of these unstable waves persist when the processes are considered in time and can be seen in solutions of system (1). The shape of the front part and its propagation speed almost exactly coincide with the shape and speed of an unstable switch-on wave. A nonstationary picture develops behind the leading wave traveling at a constant speed. Collectively, these events are responsible for the complex dynamic behavior of an excitable medium. Such complicated solutions of system (1) can be roughly categorized into two classes, ‘composite waves’ and ‘splitting waves.’ The former consist of two components, with their head parts remaining unaltered and rear ones oscillating in a complicated manner. The front edge of a splitting wave periodically emits secondary waves traveling in the opposite direction.

In this section, in order to better depict regions corresponding to different regimes in a single-parameter portrait, we consider another two-dimensional cross section of the space of ‘chemical’ parameters K_i . Specifically, the quantities K_2 and K_6 are considered variable parameters, with the remaining four parameters fixed (Table 2). (Compare parameters in Tables 1 and 2.)

Table 2

K_1	K_2	K_3	K_4	K_5	K_6	D
6.85	4–10	2.36	0.1	14.0	0.071–0.077	1.0

Figure 9 shows regions in which different stable regimes exist in the plane of parameters (K_2, K_6). There are stable autowaves for parameter values from region I (shown by

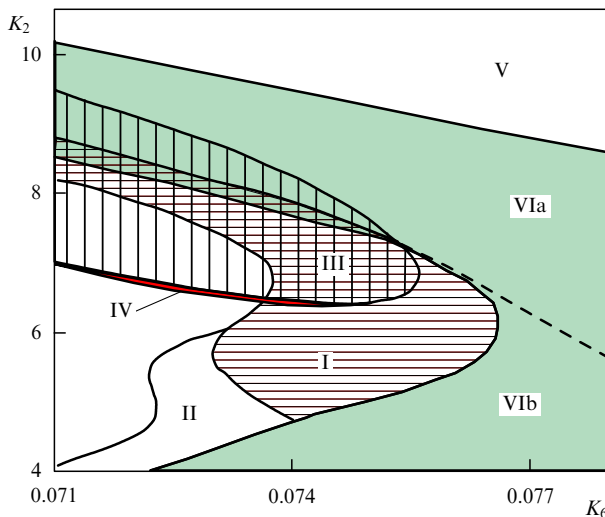


Figure 9. Regions where different regimes exist in the plane of parameters (K_2 , K_6). I — autowave region (horizontal hatching), II — oscillating autowaves, III — spatially localized standing structures — peaks (vertical hatching), IV — oscillating peaks (narrow dark region adjoining the standing peak region III from below), V — bistability region, VI — region of complex dynamic regimes (shaded). Values of the coefficients K_j are given in the text.

horizontal hatching). Region II contains autowaves with an oscillating amplitude, region III (vertical hatching) standing spatially localized structures (peaks), and region IV oscillating peaks. Region V is a bistability region having solutions in the form of stable trigger waves. Region VI is characterized by complex dynamic regimes; its subregions VIa and VIb correspond to composite and splitting waves, respectively. The lower boundary of subregion VIa is shown approximately by the dashed line. On the whole, the picture in region VI can be described as follows. Wide composite waves with nonperiodically oscillating tails are localized in the vicinity of the bistability area. The width of composite waves decreases with the distance from this area, and the lower part of subregion VIa contains narrow composite waves with a periodically oscillating tail portion. Subregion VIb located at a still greater distance from the bistability area corresponds to splitting waves. Interestingly, all the above regimes are observed within a relatively narrow range of values of the parameter K_6 defining the inhibitor lifetime.

It was found that unstable switch-on waves sometimes coexist with stable peaks or autowaves. As a rule, activation excites only peaks and autowaves, but in certain cases a composite wave is formed and oscillations of its trailing part result in stable solutions, peaks, and autowaves. Such regimes are not rough, are highly sensitive to the initial conditions, and exist in a small parameter range. A more detailed description of ‘composite waves’ is presented in Section 5.2.

5.2 Composite waves

Given parameters from subregion VIa and the standard initial conditions, excitation first spreads as a switch-on wave. The leading edge propagates at a constant speed and brings the system to the vicinity of the upper (unstable) spatially homogeneous state. The instability of this state is manifested in that the rear part of the wave picture begins to change in a complicated manner. Two types of composite waves are distinguished based on the behavior of their tail portions.

The first type is shown in Fig. 10. A local increase in the activator concentration near the left end of the segment triggers the propagation of the excitation from the boundary of the region. A *leading wave* can be identified in Fig. 10a. The region of constant values of variables (plateau) in close contact with the wave front expands for some time during motion but thereafter stabilizes. The rear part of the leading wave undergoes nonperiodic oscillations that generate pulses propagating in the opposite direction. An unstable trigger wave has the nonmonotonic profile of the first variable. The nonmonotonicity is of a trivial origin, that is, the heterocyclic trajectory of automodel equations (3) tends to their ‘upper’ singular point. This point has complex eigenvalues. When a pair of eigenvalues is close to the imaginary axis, the trajectory ‘rotates’ about the singular point. Thus, oscillations of all quantities about their limit values are inevitable. As the parameter approaches a critical value, the pair of eigenvalues comes closer to the imaginary axis and the profile of the trigger wave (unstable in evolutionary equations!) acquires a wave-like shape.

Pulses generated by the leading wave ‘try’ to develop into waves resembling the parent one. If only a single pulse is preserved, it develops into a wave identical to the leading one. Such secondary waves being generated rather frequently, the entire region behind the running primary wave turns into a chaotic activity area (Fig. 10b). When the leading wave reaches the right boundary of the segment, it interacts with the boundary and is annihilated. After that, chaotic dynamics prevails over the entire model area (Fig. 10b, $t = 10,000, 20,000$). The segment is totally filled with pulses that move unceasingly, are annihilated, give rise to new composite waves, etc. Such activity leads to the oscillations of variables at each point of space (Fig. 10c) characterized by a wide and continuous frequency spectrum (Fig. 10d); this confirms chaotic oscillation patterns. The chaotic character of the regime thus obtained is also manifested as its sensitivity to minor perturbations of the initial data.

With the progress in a downward movement into parameter region VIa (see Fig. 9), composite wave oscillations become more regular. The lower part of region VIa contains waves of the second type. An example of such waves is presented in Fig. 11a. A wave originating from the activation site at the boundary propagates at a constant speed. Its leading edge remains unaltered and the trailing one undergoes periodic oscillations. Unlike the oscillations described above, these oscillations decay without generating new pulses. The speed of the wave and the shape of its front part almost exactly coincide with the corresponding characteristics of the unstable switch-on wave existing at the same parameters. (Fig. 11b).

5.3 Splitting waves

Figure 12a illustrates the regime observed in region VIb. A wave propagating for a time with a constant speed from the activation site undergoes division; its trailing part emits a pulse that is transformed into a wave identical to the parent one but traveling in the opposite direction. As the initial wave continues to move, it gives rise to another pulse. The secondary waves also split.

A splitting wave is characterized by a two-phase change in the profile. In the first phase, the profile alters insignificantly, whereas in the division phase, the tail of the wave produces a new wave that travels in the opposite direction. The newly generated waves propagate in either direction, which leads to

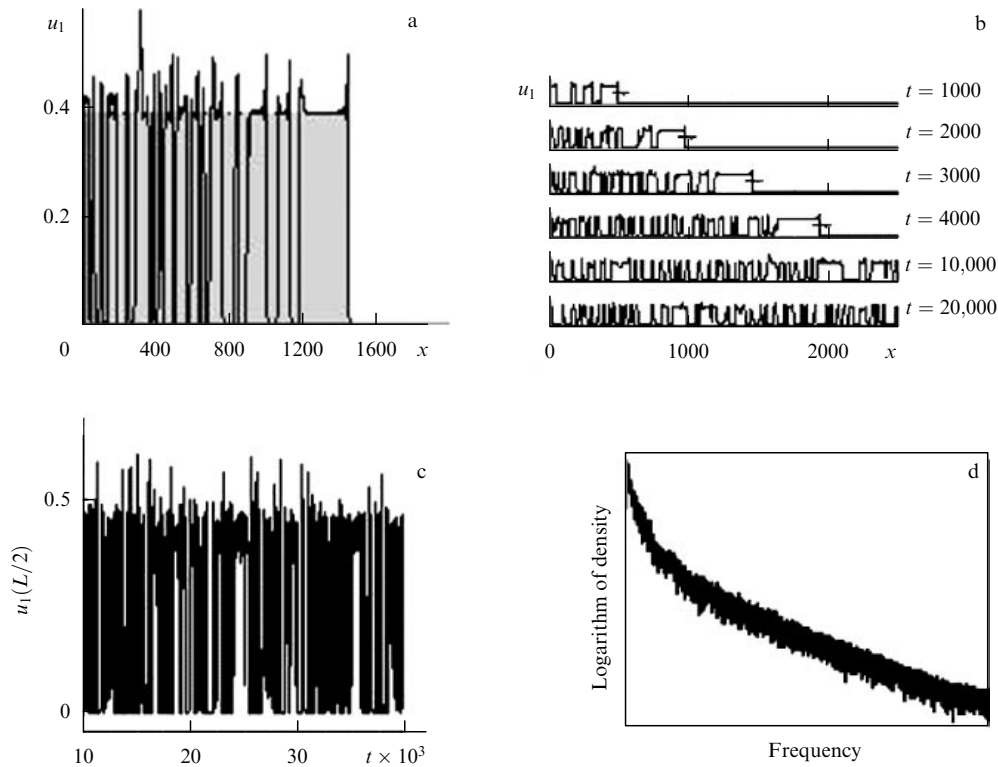


Figure 10. Type-1 composite waves. (a) Formation of a type-1 composite wave with an aperiodically oscillating rear part in response to a local increase in the activator concentration near the left boundary for the parameters $K_2 = 8.15$ and $K_6 = 0.075$. The profile of an unstable trigger wave (upper boundary of the shaded area) superimposed on the composite wave profile exactly coincides with it in the leading-edge and stationary part. (b) The shape of the composite wave depicted in Fig. (a) at different instants (indicated opposite each curve). (c) Oscillations of the variable u_1 in the center of the segment. (d) Spectrum of the oscillations shown in Fig. (c).

frequent collisions. The result of a given collision depends on the wave phase at the instant of interaction. Two interacting waves are annihilated if both are fully developed and preserve their profiles during motion (see snapshots at $t = 860$ and $t = 920$ in Fig. 12b). When one of the colliding waves is incompletely developed, they merge and give rise to a single splitting wave (see snapshots at $t = 1930$ and $t = 2000$ in Fig. 12b). If both waves are immature, they merge and give rise to two new waves propagating in opposite directions (snapshots at $t = 575$ and $t = 660$ in Fig. 12b). At large times, the entire segment is filled with continuously interacting pulses (Fig. 12b, $t = 8000$). This activity results in chaotic oscillations at each point in space. These oscillations, similarly to those under the regime described in Section 5.2, are characterized by a wide and continuous frequency spectrum (Fig. 12c). The profile of an unstable trigger wave superimposed on the profile of the splitting wave exactly coincides with it in the leading front region (Fig. 12d). Additional information is given in the caption to Fig. 12.

6. Multihump pulses

One of the most unusual regimes in blood clotting model (1) is given by multihump pulses (Fig. 13b). It has never been observed in any known model of active media; we described this regime in Ref. [11]. Multihump pulses occur when the inhibitor diffusion coefficient decreases. We recall that the solutions of system (1) considered in Sections 4 and 5 were obtained at identical diffusion coefficients D_k .

A characteristic feature of these pulses is that the amplitude and the frequency of decaying spatial oscillations

in their profiles are roughly equal irrespective of the value of the diffusion coefficient. The oscillations occur near the upper unstable spatially homogeneous state. The smaller the diffusion coefficient, the greater the decay of spatial oscillations in the profiles.

There is nothing new about complex-shaped pulses in the theory of autowaves. They were observed in the simplest (FitzHugh – Nagumo) model of an excitable medium as early as 1981 [27, 28] (the first equation is nonlinear, the second is linear and only the activator diffuses). Pulses of complex shape were also investigated in a series of studies with FHN-type models describing oxidation of CO on platinum [29, 30] (both equations are nonlinear and only the activator diffuses).

The pulses considered below remain stable even if they have many humps (see Sections 6.1 and 6.2). They are due to the disappearance of a trigger wave (unstable at the chosen parameter values). We believe this fact to be of general interest.

Sections 6.1 and 6.2 focus on the analysis of situations with equal diffusion coefficients of the activator and the catalizer ($D_1 = D_2 = 1$) as the diffusion coefficient of the inhibitor D_3 decreases from 1 to 0 at the step 0.001. In these sections, all six ‘chemical’ constants $K_1 - K_6$ are fixed: the values of K_1 , K_3 , K_4 , and K_5 are the same as in Table 2, and the values $K_2 = 7.0$ and $K_6 = 0.08$ are chosen.

6.1 Appearance of multihump pulses upon a decrease in the inhibitor diffusion coefficient

Multihump pulses exist in the model in the range of $K_1 - K_6$ parameters where the model is monostable but has two more unstable spatially homogeneous states. Figure 14 illustrates

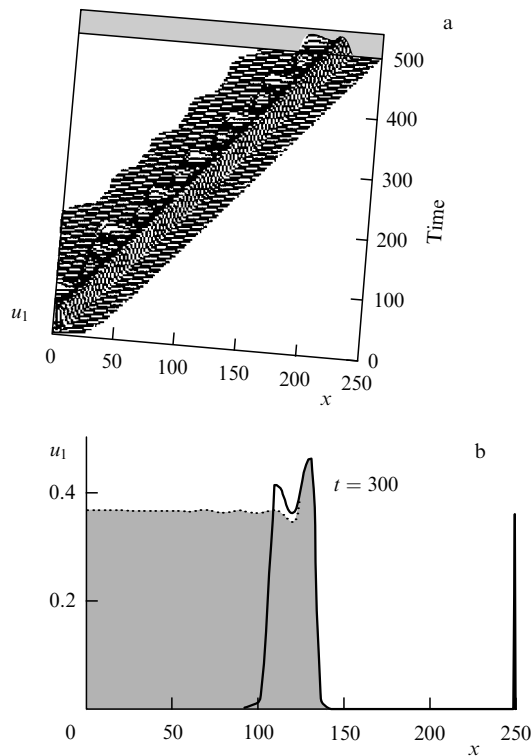


Figure 11. Type-2 composite waves. (a) Formation of a type-2 composite wave with a periodically oscillating rear part in response to a local increase in the activator concentration at the left boundary of the segment at the parameters $K_2 = 7.6$ and $K_6 = 0.075$. (b) The profile of an unstable trigger wave (upper boundary of the shaded area) superimposed on the profile of the composite wave shown in Fig. (a) exactly coincides with the leading-edge area.

the evolution of the solution of system (1) as the diffusion coefficient of the inhibitor D_3 decreases (only data for the first variable u_1 are shown). At $D_3 = 1$, the composite wave described in Section 5.1 propagates from the activation site. In the range of the diffusion coefficients D_3 from 1 to 0.702, the excitation propagates with a constant speed and an unaltered front. Both the front edge of the leading wave and the speed fairly well coincide with the characteristics of the unstable trigger front calculated at these parameters (Figs 10a and 14a). The tail of the leading wave oscillates and produces pulses that fill up the segment behind the wave. At a certain value of the diffusion coefficient of the inhibitor ($D_3 = 0.702$), the shape of the front part of the excitation zone becomes more complicated. The leading edge is immediately followed by an area with a series of alternating minima and maxima. A certain transition process ends in the formation of an autowave readily distinguishable against the background chaotic activity (Fig. 14b). This autowave is a wide excitation zone of a complex ‘multihump’ shape. All elements of this wave remain unaltered in the reference frame comoving with the wave. The number of humps decreases with decreasing the parameter D_3 (Fig. 14b–d) until the multihump wave turns into an ordinary one (see Fig. 14f where two autowaves follow each other).

Interestingly, we observed different dynamics of the formation of multihump pulses under the chosen standard initial conditions (see Section 3). Certain parameters were associated with the formation of single multihump pulses, such as a four-hump pulse (Fig. 14c) and a two-hump pulse

(Fig. 14e). At other parameters, a multihump pulse was an element of a group resembling the group of similar three-hump pulses shown in Fig. 14d. However, when an element of such a group stands for the initial data, it propagates as a single multihump pulse.

6.2 Hypothesis of the multihump pulse origin from bifurcation of trigger waves

The appearance of multihump pulses in the blood coagulation model may be attributed to bifurcation of the decay of unstable trigger waves upon a decrease in the inhibitor diffusion coefficient. In system of ordinary differential equations (3), such a wave corresponds to a ‘heteroclinic’ trajectory extending from one singular point to another, while pulses correspond to ‘homoclinic’ trajectories originating in one singular point and returning to it. The birth and disappearance of such trajectories upon a change in one or several parameters are *nonlocal* bifurcations in terms of review [31]. Such bifurcations have been extensively studied by mathematicians in the last few decades (see monographs [32, 33]; Ref. [33, Ch. 13] presents data interesting in the context of the present paper). In the theory of bifurcations, the speed of the wave, which we regarded as one of the unknowns, plays the role of a system parameter formally equal to all the others. On the plane of parameters (D_3, c), the line corresponds to the existence of a trigger wave and its end to the disappearance of the wave.

Figure 13a presents profiles of unstable trigger waves for the first variable u_1 at the diffusion coefficients $D_3 = 0.8$, $D_3 = 0.71$, and $D_3 = 0.704$. The profiles found from system (3) are positioned so as to facilitate the comparison. As the critical value $D_{3cr} = 0.703$ is approached (below which multihump pulses appear in the computation), an increase is observed in the number of spatial oscillations behind the leading edge in the vicinity of the upper state; simultaneously, their amplitude increases and the decrement of decay decreases. Newton’s method for solving Eqns (3) loses convergence near the critical value D_{3cr} ($D_3 = 0.703$). There is no solution of system (3) in the form of a trigger wave when the diffusion coefficient of the inhibitor is below the critical value; instead, solutions of the multihump pulse type appear.

These multihump solutions of Eqns (3) correspond to stationary running pulses with several humps (Fig. 14c–e) in the initial system (1); these pulses are stable, unlike trigger waves that disappear. Certainly, this important fact does not ensue from the consideration of ordinary differential equations (nor from the bifurcation theory for these equations).

Humps of these pulses correspond to oscillations of model variables about their values in the upper spatially homogeneous state. A further decrease in the inhibitor diffusion coefficient leads to bifurcations of a different type, i.e., transitions from one multihump pulse to another via changes in the hump number (Fig. 13b).

It follows from Figs 13b and 14 that a decrease in the inhibitor diffusion coefficient D_3 results in a reduced hump number in multihump pulses. In other words, the coefficient D_3 is a parameter governing the transition between pulses having different numbers of humps. However, the hump number can be just as well controlled by other parameters if multihump pulses already exist at a given value of the inhibitor diffusion coefficient, under the condition that a change in a given parameter brings the system close to its bistability region in the parameter space.

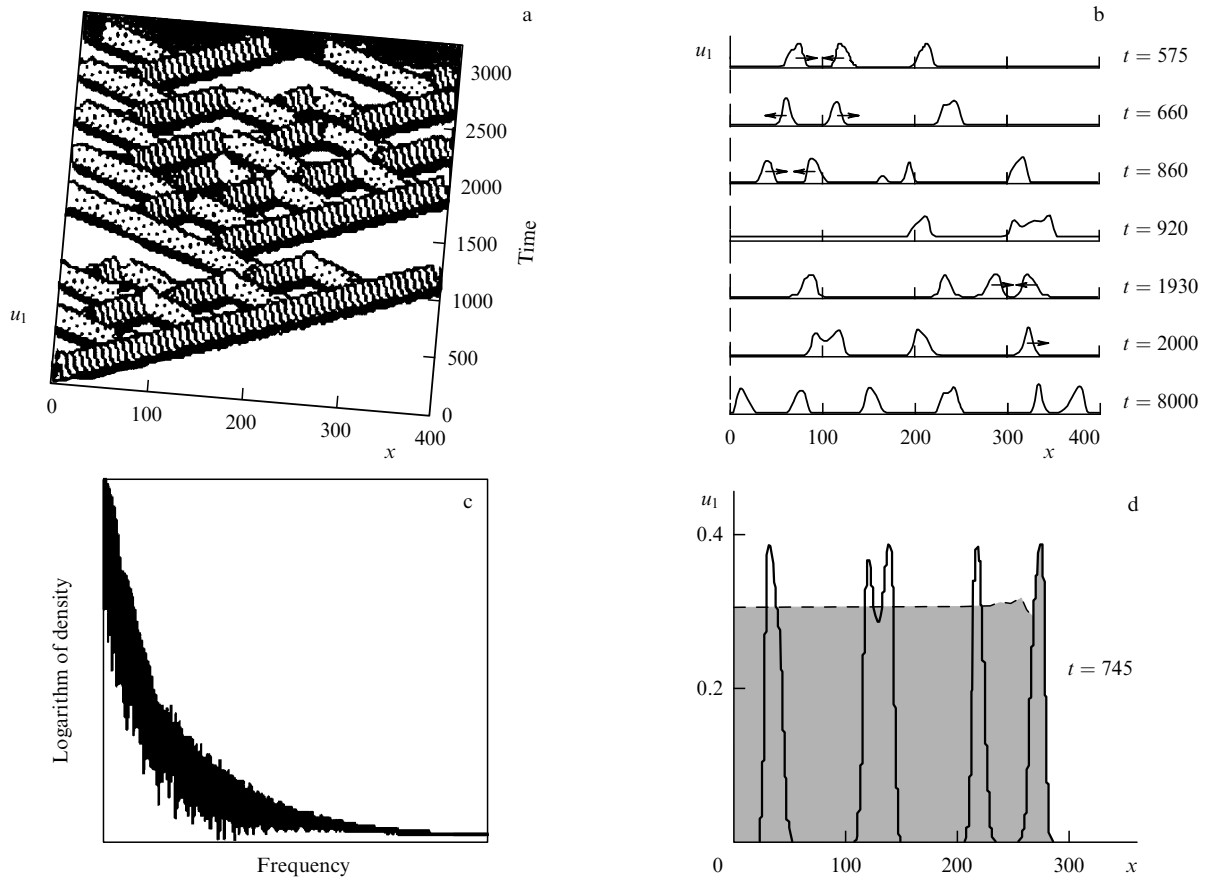


Figure 12. Splitting waves ($K_2 = 6.0$ and $K_6 = 0.077$). (a) Formation of splitting waves in response to near-boundary activation. (b) Spatial snapshots of the regime taken at the indicated instants. (c) Oscillation spectrum of the first variable recorded in the center of the segment after it is totally filled with splitting impulses. (d) Profile of an unstable trigger wave (upper boundary of the shaded area) superimposed on the profile of the splitting wave shown in Fig. (a) at $t = 745$.

As an example, we examined the evolution of system (1) upon a change in the parameter K_2 . The inhibitor diffusion coefficient was fixed as $D_3 = 0.25$ and the parameters K_1 and $K_3 - K_6$ remained unaltered. At $K_2 = 8.2$, the system was in the bistability region and the standard initial conditions led to the appearance of a switch-on wave. A decrease in the parameter K_2 resulted in the loss of stability of the upper spatially homogeneous state of the model, but this state continued to exist as an unstable one. At K_2 below 8.1, multihump pulses emerged. Any further decrease in K_2 , like that of the inhibitor diffusion coefficient, caused a sequential reduction of the number of humps until the solution turned into an ordinary autowave at $K_2 = 6.0$.

7. Conclusion

7.1 Results of the study and the general theory of active media

7.1.1 Peak formation. The study of the simplest blood coagulation model (1) as a model of excitable media revealed a few unusual complex dynamic regimes, besides the well-known ones. Also, we found time-independent solutions of this system in the form of localized peaks and showed that these stable regimes can be established in a variety of ways and at different parameter values.

As mentioned in Section 4.1, stationary spatially localized structures or peaks were described earlier in several models of

one-dimensional excitable media. However, none of these works considered the dynamics of formation of such structures. We believe that the majority of the researchers have observed the ‘natural’ course of events when the peak remains associated with the activation site whenever activation induces its formation. We confirmed this finding by verifying some of these models.

The blood coagulation model allows a new peak formation scenario. Activation first induces a quasiautowave that travels a rather large distance from the activation site, stops thereafter, and turns into a standing peak. Our model also encompasses the conventional scenario, i.e., formation of a standing peak that remains at the activation site. The two scenarios are observed at the parameters from the connected area of the existence of stable peaks in the parameter space (region 1 in Fig. 1). It suggests the same type of stationary solutions of system (1) in either case. However, the area of existence of such solutions proves inhomogeneous in that the stationary regime in its selected parts is reached in a different way.

7.1.2 Overlapping regions. The blood coagulation model in (1) also contains solutions in the form of traveling waves of constant shape (autowaves) characteristic of excitable media. The region where autowaves exist in the parameter space is region 2 in Fig. 1. An interesting feature of model (1) is the intersection of region 1 (stable peaks) and region 2 (stable autowaves). The overlapping area is dominated by autowaves

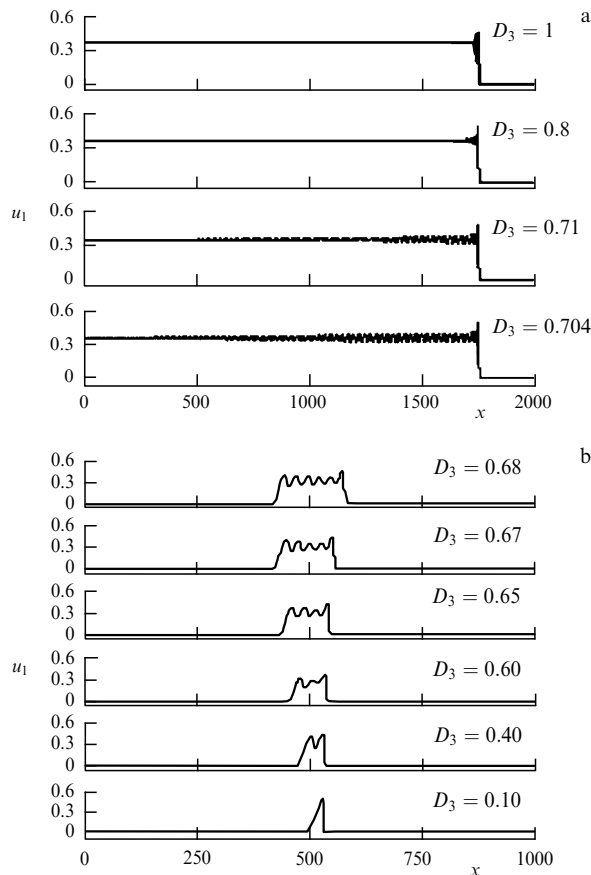


Figure 13. Comparison of profiles of unstable switch-on waves and stable multihump pulses upon a change in the inhibitor diffusion coefficient D_3 . (a) Profiles of unstable trigger waves at the shown D_3 values. (b) Profiles of stable multihump pulses.

induced by standard initial activation. The coexistence of stable peaks and autowaves has not been described before. It was inferred from the analysis of simple models that these regimes were mutually exclusive. Such a conclusion might have been prompted by the fact that the solutions in the form of peaks in simple models of active media were usually found at a ratio of the activator and inhibitor diffusion coefficients below unity, whereas autowave solutions normally require it to be higher than that. In our model, the peaks and the autowaves occur at identical diffusion coefficients. Therefore, the respective solutions may have adjacent spatial parameter areas and may even coexist at identical parameter values.

Having discovered coexisting stable peaks and autowaves in model (1), we also identified them in other models. We studied the system of two equations proposed by Pertsov [34, 35] by inserting a nonzero diffusion coefficient in the equation for the inhibitor. This set of equations is actually a modified FHN model containing a piecewise-linear function in the equation for the activator and a discontinuous right-hand side in the second equation. In such a system, stable traveling pulses and stationary peak-like solutions may also coexist at equal diffusion coefficients. By varying the model parameters, we obtained all the aforementioned dynamic regimes except that of multihump pulses. Some of them were observable only at unequal diffusion coefficients.

In a later study, we found peak formation regimes similar to those described in the preceding paragraphs also in the model proposed in [18].

7.1.3 Bifurcation memory. We analyzed a new scenario of peak formation from a traveling autowave that stops at a distance from the activation site (see Sections 4.2 and 4.3) and came to the conclusion that this phenomenon is related to the so-called ‘bifurcation memory.’ This term was proposed in Ref. [36] to describe the fact that solutions of a system of differential equations (when the boundary of the region in which they exist is crossed in the parameter space) retain similarity with the already nonexistent type of solutions as long as the variable parameter values insignificantly differ from the limit value.

In mathematical models describing processes in time, this fact is known as a corollary of the theorem on continuous dependence of solutions of differential equations (on a finite time interval) on their parameters; from this standpoint, it is not fundamentally new.

In our model, autowave solutions disappear after a change in parameters as a result of merging between the families of stable and unstable autowaves; neither the speed nor the amplitude of the waves tends to zero in this case. Therefore, the response of the system to standard activation in the immediate proximity to the boundary (in the external vicinity of the autowave region) is still similar to the response inside this region, and the excitation first propagates as a traveling pulse. Thereafter, the solution relaxes toward one of the stable solutions existing in region I (a stable peak).

A similar situation occurs near those parts of the boundary of the autowave region that adjoin other regions in the parameter space, e.g., near the boundary between regions 2 and 5 (see Fig. 1). In this case, too, the standard excitation first causes a propagating quasiautowave that afterwards relaxes to a trivial (spatially homogeneous) stable state. A similar picture is observed at the boundaries of the region of stable switch-on waves (in the lower part of area B in Fig. 1). The initial stage of stable peak formation at the boundary common to a switch-on wave and stable peak regions resembles the propagation of a switch-on wave. The excitation area first expands and thereafter narrows to a peak at the activation site. In all cases, we observed effects of ‘bifurcation memory’ in our model near those parts of the boundaries between parameter regions where bifurcation of merging occurred.

7.1.4 ‘Survival’ of unstable solution sites. In Section 5, the following important fact was emphasized in the discussion of complex dynamic regimes feasible in model (1). Switch-on waves are unstable at the parameters corresponding to complex dynamic regimes (area VI in Fig. 9) and cannot therefore appear in time-dependent problem (1). Indeed, these waves are not observed as a whole, but their leading edges ‘survive’ and exist infinitely long. The profiles of the head part of composite (or splitting) waves are not strictly stationary, but their time-dependent oscillations near the leading edge are very weak and practically unapparent.

This is by no means a unique feature of the problem under consideration. The stationary (in a broad sense) regimes in distributed systems should not necessarily escape observation after they have lost stability; the resulting instability may manifest itself differently in different space areas and is sometimes insignificant.

For example, such is the case in the Gray–Scott model [37], given by two differential equations with the simplest chemical terms. At equal diffusion coefficients, the parameter plane of this system exhibits an area in which the set of

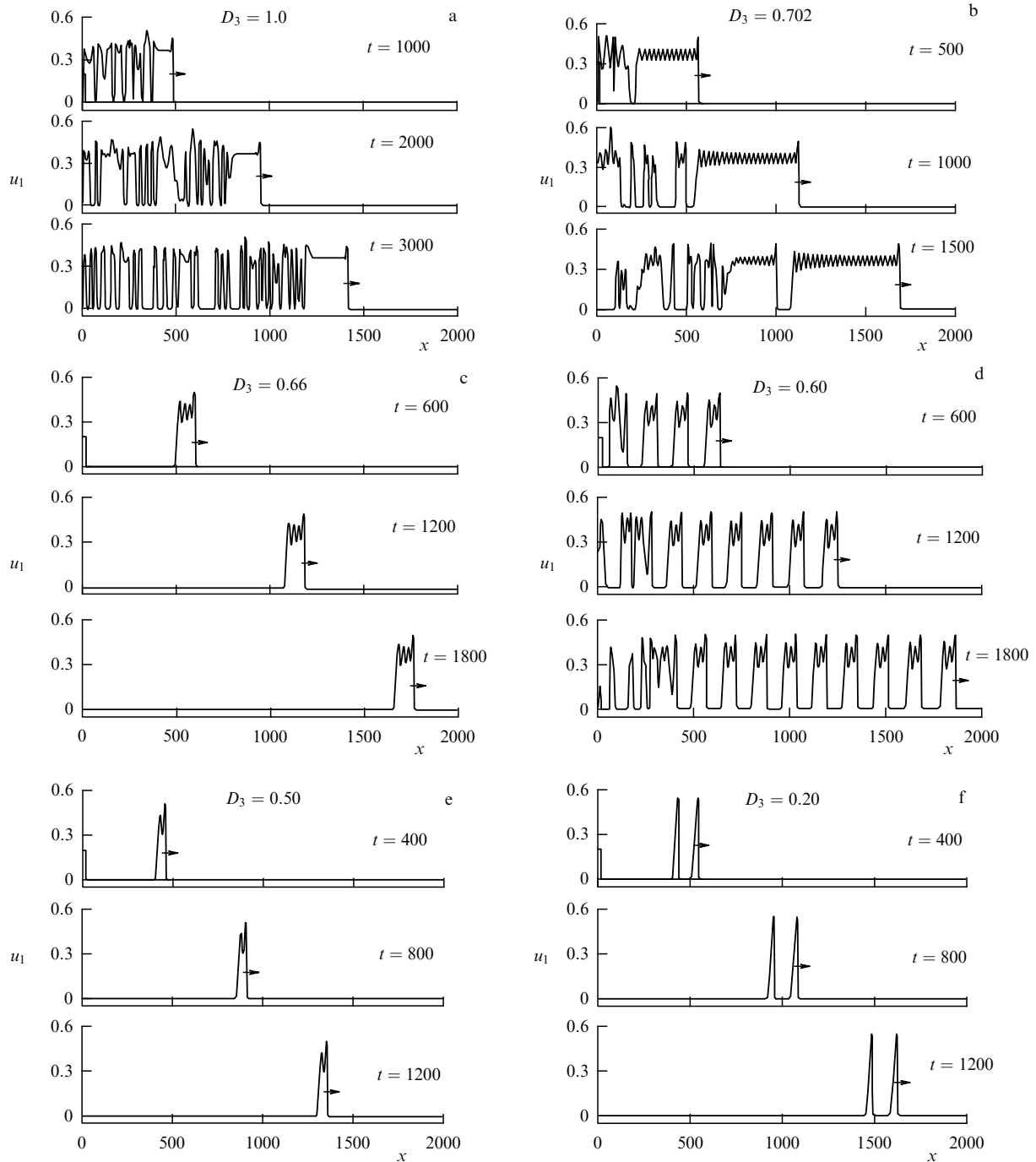


Figure 14. Snapshots taken at different instants for the dynamic regimes developing at the values of the inhibitor diffusion coefficient D_3 shown in the figure in response to activation near the left boundary.

equations has three spatially homogeneous solutions, one stable and two unstable. Part of this area exhibits ‘chaotic’ regimes [38] similar to those described in Section 5. In addition, we here also observed a high degree of coincidence between the head profiles of a propagating excitation wave and an unstable switch-on wave. As many other models of active media, our model is bistable at certain parameter values and monostable at others.

Unstable switch-on waves are responsible for the formation of multihump pulses. Of special interest is a series of bifurcations arising from a change in the parameter, e.g., the diffusion coefficient, and manifested as an altered number of

humps that decreases with decreasing the diffusion coefficient. It seems that a given parameter value should correspond to a definite number of humps. However, this is not the case, and solutions with different hump numbers coexist at some parameter values. A detailed study of this bifurcation is underway and may lead to unexpected results.

7.1.5 A wealth of solutions near the state-change boundary. Of special interest is the fact that all complex dynamic regimes observed in cross sections of the parameter space (see, e.g., Figs 1 and 9) exist along the boundary between mono- and bistability regions. Regions of autowaves, complex pulses,

and other dynamic regimes adjoin this boundary from the monostability side. Accordingly, there are different types of solutions near this boundary in the known models of active media with two equations (such as the Gray–Scott model and models of the FHN type [37, 38]). The area in the vicinity of the boundary between mono- and bistability regions appears to be rich in all kinds of spatially heterogeneous stationary and dynamic regimes. It seems that transition from a single homogeneous lower state to its coexistence with the equipotent upper state filling the entire space looks like a smooth process. In the course of development, the upper state may be partly expressed in the form of spatially localized, standing or intricately moving solutions. We think that this observation may constitute a heuristic principle in the search for interesting regimes in complex models of the reaction–diffusion type.

7.2 Relation of the results to the current blood coagulation concepts

Blood coagulation starts from the synthesis of large amounts of thrombin near the injured wall of a vessel. Thrombin, in turn, triggers formation of factors required for both its spatial distribution and the termination of its production. The first variable in the model being considered describes thrombin concentration.

Thus, the initial conditions that we called standard (see Section 2) simulate the real situation. The spatial dynamics of blood coagulation in experiment are very similar to the model dynamics near the left boundary of the autowave region; specifically, the excitation first propagates as an autowave and thereafter transforms into a peak and decays. In a more complicated blood clotting model [39], the time integral of thrombin concentration describes the clot size and density in the first approximation. In experiment, a clot develops at a constant rate over a long period, after which the growth stops [3]. This process corresponds to the propagation of a thrombin pulse with an approximately constant speed and its eventual disappearance. A stable thrombin peak suggests that the density at the clot periphery should infinitely increase after the termination of the growth. Certainly, no infinite increase is observed either in experiment or in a complete model. The infinite increase is the assumption, made in constructing the simplified model, that concentrations of the precursors of fibrin, thrombin, and other clotting factors do not change during the coagulation process. In a more complete model, the peaks are quasistationary, i.e., exist much longer than the transition process. Such a clot growth regime is also observed in experiment. The clot stops developing, but its edges become increasingly denser (unpublished data obtained by Ataullakhanov and co-workers at the Center for Hematology).

Regimes under which a thrombin impulse first propagates, then stops and transforms into a standing peak or decays are observed in model (1) only in a narrow range of parameter values near the boundary of the autowave region. In model (1), these regimes represent manifestation of the ‘bifurcation memory’ about the true autowave regime. It is hardly possible that the clot growth strongly depends on the parameters of the blood coagulation system and the condition of the body at large. It is even less likely that the clotting system always functions under conditions corresponding to those at the boundary of the place of origin of the regime in which the thrombus can grow infinitely leading to a fatal outcome. Evidently, model (1) does not account for

certain essential links and factors ensuring the relative independence of the coagulation process from parameter values. First, consideration of only three biochemical parameters of this process is clearly insufficient. It must be borne in mind that clotting occurs in the blood flow and that vascular walls are not neutral but actively involved in the coagulation process [40]. The very first attempts to take these two factors into account indicate [41] that they actually have a marked effect on process dynamics.

The real dimensions of blood vessels are small compared to the characteristic size of the above waves and structures. Therefore, talk of an established real blood coagulation regime sounds like a strained interpretation. Certainly, this complicates consideration of blood clotting dynamics; it is then even more remarkable that a rather simple model describes the main features of the coagulation process fairly well. Moreover, it allows revealing and investigating a number of quite new dynamic regimes and thus substantially extending our knowledge of reaction–diffusion systems.

This work was partly supported by the Russian Foundation for Basic Research, grant nos 00-04-48855-a, 03-04-48388-a, and 06-04-48426-a, a grant from the Russian–French scientific cooperation program PICS, no. 05-01-22001, and grant no. MK-7062.006.4 from the President of the Russian Federation.

References

1. Ataullakhanov F I, Guriya G T *Biofizika* **39** 89 (1994) [*Biophys.* **39** 89 (1994)]
2. Ataullakhanov F I, Guriya G T, Safroshkina A Yu *Biofizika* **39** 97 (1994) [*Biophys.* **39** 99 (1994)]
3. Ataullakhanov F I et al. *Biochim. Biophys. Acta (BBA)–Gen. Subjects* **1425** 453 (1998)
4. Zarnitsina V I, Pokhilko A V, Ataullakhanov F I *Thromb. Res.* **84** 225 (1996)
5. Zarnitsina V I, Pokhilko A V, Ataullakhanov F I *Thromb. Res.* **84** 333 (1996)
6. Zarnitsina V I et al. *Chaos* **11** 57 (2001)
7. Ataullakhanov F I et al. *Int. J. Bifurcat. Chaos* **12** 1985 (2002)
8. Ataullakhanov F I *Usp. Fiz. Nauk* **172** 671 (2002) [*Phys. Usp.* **45** 619 (2002)]
9. Lobanova E S, Shnol E E, Ataullakhanov F I *Phys. Rev. E* **70** 032903 (2004)
10. Lobanova E S, Ataullakhanov F I *Phys. Rev. Lett.* **91** 138301 (2003)
11. Lobanova E S, Ataullakhanov F I *Phys. Rev. Lett.* **93** 098303 (2004)
12. Godunov S K *Usp. Mat. Nauk* **16** (3) 171 (1961)
13. Bakhvalov N S, Zhidkov N P, Kobel'kov G M *Chislennyye Metody (Numerical Methods)* (Moscow: Nauka, 1987) Ch. 9
14. Ascher U M, Mattheij R M, Russell R D *Numerical Solution of Boundary Value Problems for Ordinary Differential Equations* (Englewood Cliffs, NJ: Prentice Hall, 1988)
15. Koga S, Kuramoto Y *Prog. Theor. Phys.* **63** 106 (1980)
16. Field R J, Burger M (Eds) *Oscillations and Traveling Waves in Chemical Systems* (New York: Wiley, 1985)
17. Kerner B S, Osipov V V *Avtosolitony: Lokalizovannyye Sil'noneravnovesnyye Oblasti v Odnorodnykh Dissipativnykh Sistemakh (Autosolitons: Localized Strongly Non-Equilibrium Regions in Homogeneous Dissipative Systems)* (Moscow: Nauka, 1991) [Translated into English: *Autosolitons: a New Approach to Problems of Self-Organization and Turbulence* (Dordrecht: Kluwer Acad., 1994)]
18. Ito A, Ohta T *Phys. Rev. A* **45** 8374 (1992)
19. Schütz P, Bode M, Gafichuk V V *Phys. Rev. E* **52** 4465 (1995)
20. Zaikin A N “Formirovaniye, rasprostraneniye i vzaimodeystviye eksitonov (avtovoln-kvazichastits) v aktivnoi srede” (“Formation, distribution, and interaction of excitons (autowaves-quasiparticles) in an active medium”), Preprint (Pushchino: Pushchino Scientific Center of the Russian Academy of Sciences, 1993)
21. Zaikin A N *Fiz. Mysl' Rossii* (1) 54 (1995)

22. Schenk C P et al. *Phys. Rev. Lett.* **78** 3781 (1997)
23. Schenk C P et al. *Phys. Rev. E* **57** 6480 (1998)
24. Poptsova M S “Transformatsiya avtovoln v lokal’no-neodnorodnykh aktivnykh sredakh” (“Transformation of autowaves in locally heterogeneous media”), Thesis Cand. Phys-Math. Sci. (Moscow: Physics Department, Moscow State Univ., 2004)
25. Or-Guil M et al. *Phys. Rev. E* **57** 6432 (1998)
26. Hagberg A, Meron E *Nonlinearity* **7** 805 (1994)
27. Kuznetsov Yu A, Panfilov A V “Stokhasticheskie volny v sisteme Fitts-Kh’yu–Nagumo” (“Stochastic waves in the FitzHugh–Nagumo system”), Preprint (Pushchino: Scientific Center of Biological Research of the USSR Academy of Sciences, 1981)
28. Kuznetsov Yu A *Elements of Applied Bifurcation Theory* (Applied Math. Sci., Vol. 112) 2nd ed. (New York: Springer, 1998) Subsect. 6.3
29. Krishnan J et al. *Comput. Meth. Appl. Mech. Eng.* **170** 253 (1999)
30. Or-Guil M et al. *Phys. Rev. E* **64** 046212 (2001)
31. Arnol’d V I et al. “Teoriya bifurkatsii” (“Bifurcation theory”), in *Itogi Nauki i Tekhniki* (Recent Progress in Science and Technology) (Ser. Sovremennye Problemy Matematiki. Fundamental’nye Napravleniya (Current Problems in Mathematics. Basic Research) Vol. 5 (Dynamical Systems 5), Eds V I Arnol’d, R V Gamkrelidze) (Moscow: VINITI, 1986) p. 5 [Translated into English: Arnols V I et al. “Bifurcation Theory”, in *Dynamical Systems V: Bifurcation Theory and Catastrophe Theory* (Encyclopedia of Mathematical Sciences, Vol. 5) (Berlin: Springer, 1994) p. 1]
32. Il’yashenko Yu, Veigu Li *Nelokal’nye Bifurkatsii* (Nonlocal Bifurcations) (Moscow: MTsNMO–CheRo, 1999)
33. Shilnikov L P et al. *Methods of Qualitative Theory in Nonlinear Dynamics* (World Scientific Ser. on Nonlinear Sci., Ser. A, Vol. 5) Pt. I, II (Singapore: World Scientific, 1998, 2001)
34. Ermakova E A, Pertsov A M *Biofizika* **31** 855 (1986)
35. Pertsov A M, Ermakova E A, Shnol E E *Physica D* **44** 178 (1990)
36. Nishiura Y, Ueyama D *Physica D* **130** 73 (1999)
37. Gray P, Scott S K *Chem. Eng. Sci.* **39** 1087 (1984)
38. Merkin J H et al. *Phys. Rev. Lett.* **76** 546 (1996)
39. Pantelev M A et al. *Biophys. J.* **90** 1489 (2006)
40. Ataullakhanov F I, Pantelev M A *Pathophysiol. Haemos. Thromb.* **34** 60 (2005)
41. Ermakova E A, Pantelev M A, Shnol E E *Pathophysiol. Haemos. Thromb.* **34** 135 (2005)